



OPEN

New dual inducible cellular model to investigate temporal control of oncogenic cooperating genes

Matthew R. Kent¹, Amanda N. Jay^{1,2} & Genevieve C. Kendall^{1,3}✉

The study of cooperating genes in cancer can lead to mechanistic understanding and identifying potential therapeutic targets. To facilitate these types of studies, we developed a new dual-inducible system utilizing the tetracycline- and cumate-inducible systems driving HES3 and the PAX3::FOXO1 fusion-oncogene, respectively, as cooperating genes from fusion-positive rhabdomyosarcoma. With this model, we can independently induce expression of either HES3 or PAX3::FOXO1, as well as simultaneously induce expression of both genes. This new model will allow us to further investigate the cooperation between HES3 and PAX3::FOXO1 including the temporal requirements for genetic cooperation. Functionally, we show that dual-induction of PAX3::FOXO1 and HES3 modifies sphere formation in a HEK293T-based system. More broadly, this lentiviral dual-inducible system can be adapted for any cooperating genes (overexpression or knockdown), allowing for independent, simultaneous, or temporally controlled gene expression.

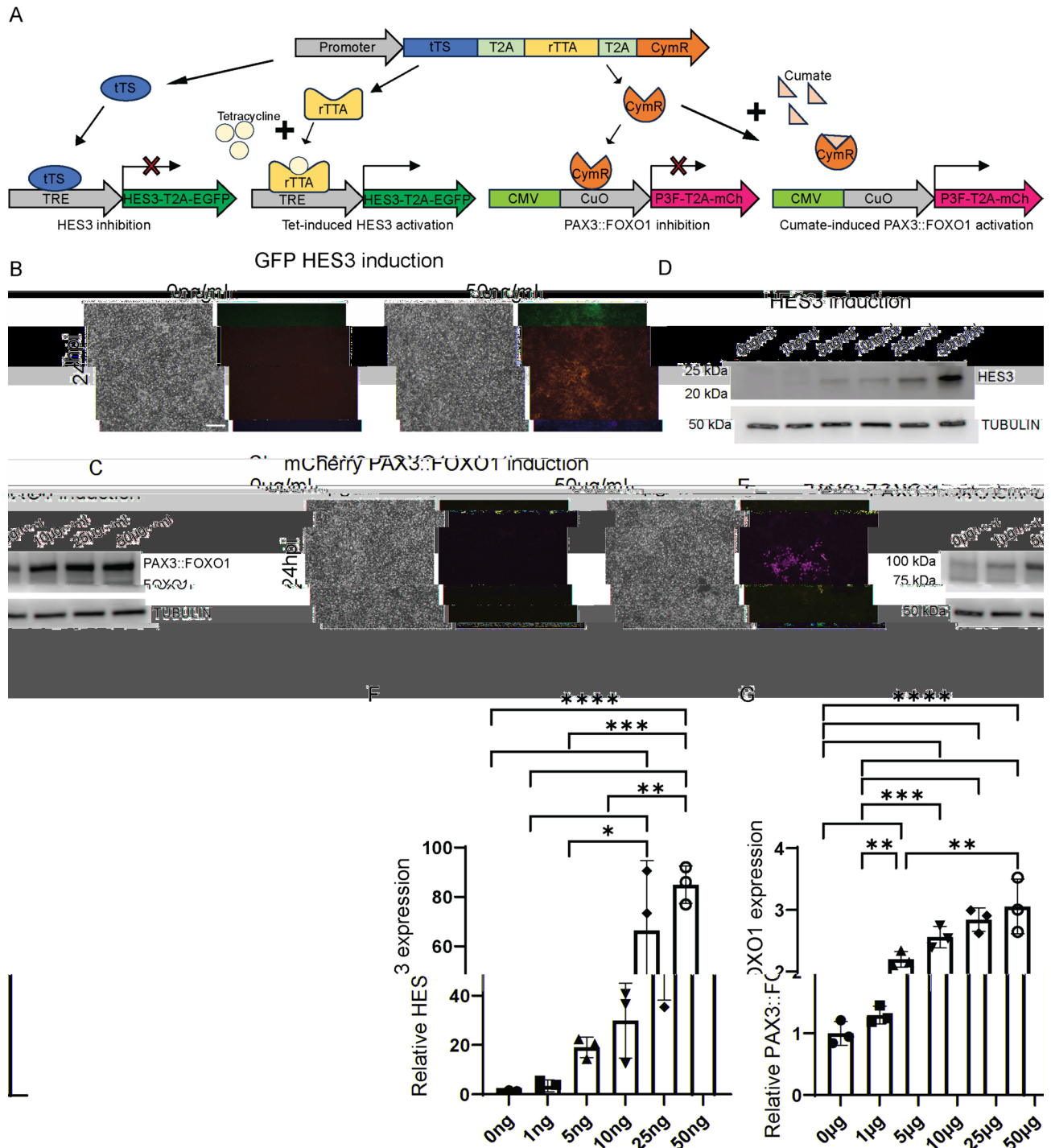
Keywords Cooperating genes, Fusion-oncogene, Inducible expression, Tetracycline-inducible expression, Cumate-inducible expression, Temporal control

Functional genomics is an important strategy for understanding oncogenesis and therapeutic vulnerabilities. Loss and gain-of-function approaches in a cell culture context can be leveraged to define genetic cooperation and the resulting phenotypic outcomes. To this end, overexpression or knockdown of putative oncogenes and cooperating genes has led to important discoveries regarding how they may be functioning in cancer cells^{1–5}. However, typically, this type of modeling does not account for critical factors in the tumorigenic process, including timing of expression, the level and duration of expression, or cessation of expression. For these types of questions, an inducible system such as the tetracycline-inducible system or the cumate-inducible system is much better suited. Additionally, combining these systems to have temporal control over multiple genetic events is challenging because of the required number of vectors to introduce into cells, as shown in a previous study in which the cumate and tetracycline expression systems were used in mixed cell populations rather than the same cell line⁶.

The tetracycline-inducible system utilizes either tetracycline or a derivative, such as doxycycline, to reversibly induce transcriptional activation or repression⁷. The Tet-On system uses a combination of a tetracycline-controlled transcriptional silencer (tTS), which silences TRE promoters in the absence of tetracycline, and a reverse tetracycline transactivator (rtTA), which is only capable of binding the TRE in the presence of tetracycline⁷. The cumate repressor system utilizes the bacterial cumate repressor (CymR), which binds to the cumate operon (CuO) in the absence of cumate⁸. The tetracycline-inducible and cumate-inducible systems are each meant to be used with a single gene at a time given the packaging limitations for vectors backbones. Thus, these systems are challenging to use for complex studies of gene cooperation.

In this study, we combined these two systems in a single cell line via a series of vectors introduced by lentiviral transduction. We engineered the regulatory tTS and rtTA for the Tet-On system and the cumate repressor CymR, all separated by viral T2A sequences, to be in one vector. In a second vector, we designed a tetracycline-inducible HES3 with EGFP separated by a viral T2A sequence. In the third vector, we designed a cumate-inducible PAX3::FOXO1 with mCherry separated by a viral T2A sequence (Fig. 1A). The rationale for generating this system is motivated by our previous work in PAX3::FOXO1 rhabdomyosarcoma, an aggressive solid tumor that presents in children. Previously, we used a cross-species comparative oncology approach to identify HES3 as a cooperating gene in the disease. We found that HES3 locks cells in an immature cell state, and that its

¹Center for Childhood Cancer Research, The Abigail Wexner Research Institute, Nationwide Children's Hospital, 575 Children's Crossroad, Columbus, OH 43215, USA. ²Department of Molecular Genetics, The Ohio State University, Columbus, OH 43210, USA. ³Department of Pediatrics, The Ohio State University College of Medicine, Columbus, OH 43215, USA. ✉email: Genevieve.Kendall@NationwideChildrens.org



overexpression is predictive of reduced overall survival in patients³. Now, we have developed a complementary cell-based system to functionally assess the requirements for HES3 in the disease. By utilizing both the Tet-On and cumate repressor systems in a single cell line, we generated a new system to investigate potential cooperation of PAX3::FOXO1 and HES3, with the capacity to independently control the level and timing of expression of each gene.

Materials and methods

Cell culture

HEK293T cells (CRL-3216, ATCC, RRID: CVCL_0063) were grown in Dulbecco's modified Eagle's media with GlutaMAX (DMEM, 10569044, Gibco) supplemented with 10% FBS, 1 × Penicillin/Streptomycin, and 10 mM glutamine. Cells were passaged every 3–4 days with TrypLE (12604013, Gibco). Cells were authenticated by STR and tested for mycoplasma annually through Genetica Inc a subdivision of LabCorp.

◀Fig. 1. Anhydrotetracycline induction of HES3 and cumate induction of PAX3::FOXO1 is titratable. Schematic of tetracycline and cumate induced expression of HES3 and PAX3::FOXO1 (A). Dual inducible HEK293T cells (referred to as 293Tii) were plated on 12-well plates at a density of 250,000 cells per well. After overnight adherence, cells were treated with titrating amounts of either: anhydrotetracycline at 0, 1, 5, 10, 25, or 50 ng/ml; or cumate at 0, 1, 5, 10, 25, or 50 µg/ml. Shown are representative images of cells imaged at 24 h post-induction (hpi) on a Leica DMI microscope with a 10× objective for GFP fluorescence (HES3) or mCherry fluorescence (PAX3::FOXO1) and then harvested for western blotting (B,C). Brightfield images were exposed for 5 ms. GFP and mCherry images were exposed for 2 s. Scale bar is 500 µm. (D,E) Cells were lysed, and then 20 µg of protein was loaded into each well of a 4–15% gradient gel. After transferring to a PVDF membrane, the membrane pieces were blotted with either a HES3 primary antibody (D), FOXO1 primary antibody that recognizes the PAX3::FOXO1 fusion and endogenous FOXO1 (E), or TUBULIN primary antibody (D,E). (F,G) Quantification of western blot data for HES3 (F) or PAX3::FOXO1 (G) protein expression. Shown is the ratio of HES3 or PAX3::FOXO1 expression normalized to TUBULIN, and presented as the fold-change to no drug treatment (far left on both graphs). Each point represents a biological replicate (n = 3 for each condition). The error bars represent the mean ± standard deviation. The p values were calculated using a one-way ANOVA followed by Tukey's multiple comparisons post hoc test. This was repeated three times. Anhydrotetracycline p-values: 0 ng vs 25 ng, p = 0.00081; 0 ng vs 50 ng, p = 0.00008; 1 ng vs 25 ng, p = 0.00112; 1 ng vs 50 ng, p = 0.0001; 5 ng vs 25 ng, p = 0.0108; 5 ng vs 50 ng, p = 0.00075; 10 ng vs 50 ng, p = 0.00348. Cumate p-values: 0 µg vs 5 µg, p = 0.0005; 0 µg vs 10 µg, p = 0.00004; 0 µg vs 25 µg, p = 0.00001; 0 µg vs 50 µg, p = 0.000002; 1 µg vs 5 µg, p = 0.0055; 1 µg vs 10 µg, p = 0.0003; 1 µg vs 25 µg, p = 0.00004; 1 µg vs 50 µg, p = 0.00001; 5 µg vs 50 µg, p = 0.008. HES3 and associated TUBULIN blot were cut from the same membrane prior to primary antibody hybridization. PAX3::FOXO1 and associated TUBULIN blot were cut from the same membrane prior to primary antibody hybridization. Western blots have been cropped from original and the uncropped blots are presented in Supplemental Fig. 7. Acronyms: tTS, tetracycline-controlled transcriptional silencer; rtTA, reverse tetracycline transactivator; TRE, tetracycline response element promoter; cymR, cumate repressor; cuO, cumate operator site; P3F, PAX3::FOXO1; mCh, mCherry.

Lentiviral plasmids

To design the plasmid containing the Tet-On regulatory proteins and the cumate repressor, we used VectorBuilder's Tet Regulatory Protein Expression Lentiviral Vector as a base, which contains both the tTS and rtTA proteins linked via a T2A sequence. We then added the CymR sequence directly downstream of this linked by a second T2A sequence. Additionally, this plasmid contains a blasticidin resistance gene for antibiotic selection. The plasmid map is available in Supplemental Figure S1.

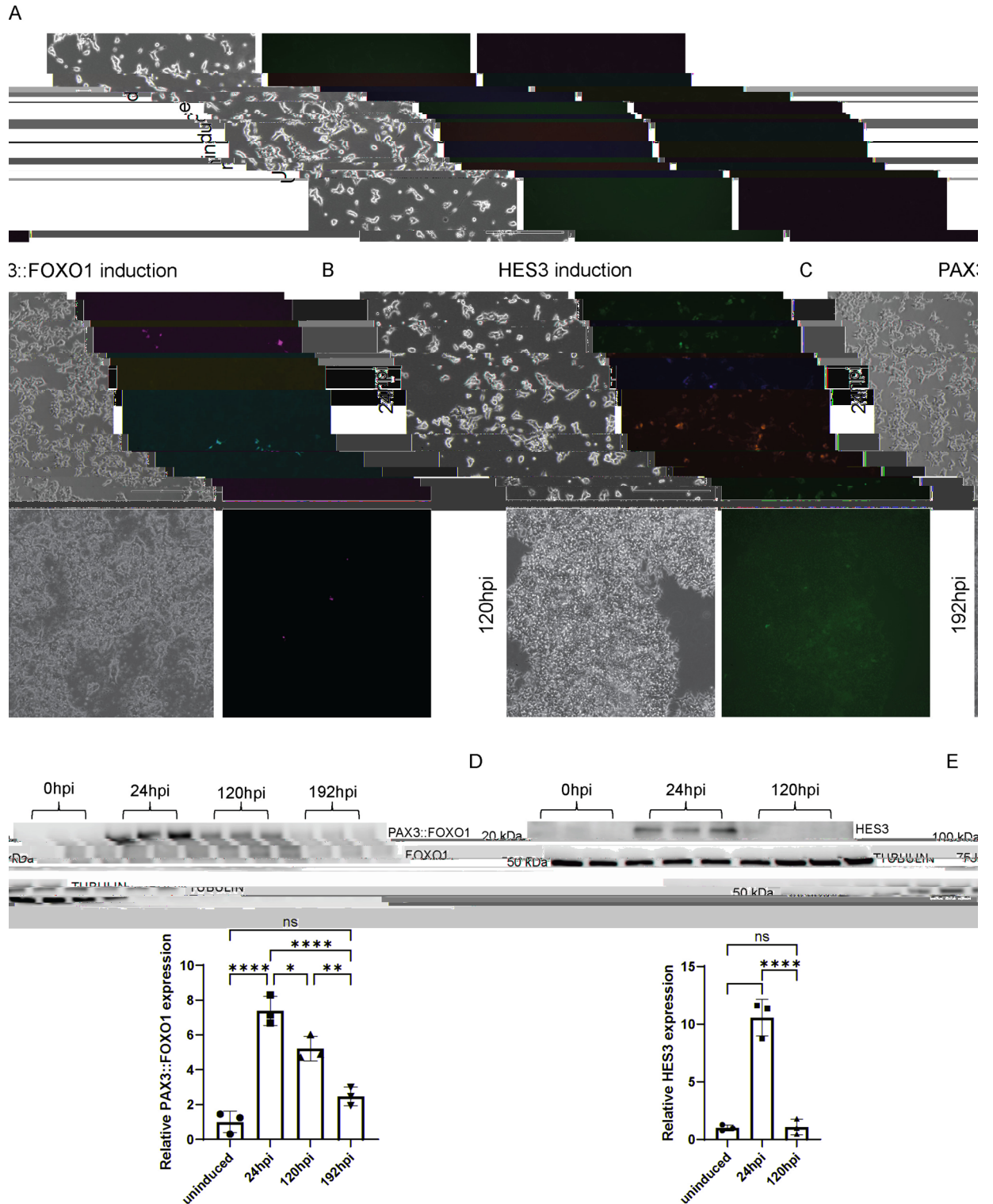
To design the plasmid containing the tetracycline-inducible gene, we used VectorBuilder's Mammalian Tet Inducible Gene Expression Lentiviral Vector as a base, adding the coding sequence for either a multicloning site (MCS) or human HES3 with no stop codon directly downstream of the TRE sequence, linked to EGFP with a T2A sequence. Additionally, this plasmid contains a puromycin resistance gene for antibiotic selection. The plasmid maps are available in Supplemental Figure S2 for MCS version and Supplemental Figure S3 for HES3 version.

To design the plasmid containing the cumate-inducible gene, we used VectorBuilder's Mammalian Tet Inducible Gene Expression Lentiviral Vector as a base. Then we replaced the TRE sequence with a CMV promoter and CuO sequence, adding the coding sequence for either a multicloning site (MCS) or human PAX3::FOXO1 with no stop codon directly downstream of the TRE sequence, linked to mCherry with a T2A sequence. Additionally, this plasmid contains a hygromycin resistance gene for antibiotic selection. The plasmid maps are available in Supplemental Figure S4 for MCS version and Supplemental Figure S5 for PAX3::FOXO1 version.

These plasmids were generated and packaged into lentivirus by VectorBuilder with a minimum virus titer of 1×10^8 TU/mL.

Lentiviral transduction

HEK293T cells were transduced with each vector sequentially to prevent potential cytotoxicity from PAX3::FOXO1 expression. The multiplicity of infection (MOI) used for each vector was 5. For transduction, 10,000 cells were plated on a 6-well plate with 2 mL of culturing media and allowed to adhere for 16 h overnight. Then, transduction media was made with 80% culturing media, 20% TransDux MAX Lentivirus Transduction Enhancer (LV860A-1, System Biosciences), and 0.5% TransDux (LV860A-1, System Biosciences). 72 h after transduction, transduction media was removed and fresh culturing media was added with selection antibiotic. For the tTS/rtTA/CymR vector (developed in this study, Supplemental Figure S1), 3 µg/mL of blasticidin (A1113903, Fisher Scientific) was used for selection. For the TRE:HES3-T2A-EGFP vector (developed in this study, Supplemental Figure S3), 1 µg/mL of puromycin (A1113803, Fisher Scientific) was used for selection. For the CMV-CuO:PAX3::FOXO1-T2A-mCherry vector (developed in this study, Supplemental Figure S5), 300 µg/mL of hygromycin (10-687-010, Fisher Scientific) was used for selection. Each antibiotic was used for selection of its respective construct for two weeks post transduction. Then the next construct and drug selection were sequentially added. The only time a combination of drugs was included (all three) was in the two weeks after FAC sorting. After the two week selection periods for vector constructs, the drugs (puromycin, hygromycin, blasticidin) were not included in the media during experiments. These concentrations were determined by performing an antibiotic selection kill-curve. Briefly, 10,000 cells were plated in each well of a 96-well plate in growth media. In triplicate, titrated concentrations of blasticidin, puromycin, or hygromycin were added to each well every two days for six days total. After six days of exposure to antibiotic, crystal violet staining was done. After aspirating out all growth media, the cells were fixed with 4% paraformaldehyde (50-276-31, Fisher Scientific) for 15 min at room temperature and then washed with $1 \times$ PBS. After aspirating out the PBS, crystal violet stain



was added for 5 min (250 mg crystal violet (C0775, Sigma-Aldrich) added to 100 mL of 20% methanol). The crystal violet stain was then removed, and the plate was gently washed by submerging in a container of still tap water, and repeated once with fresh tap water. The plate was then allowed to air dry. To extract and quantify, 10% glacial acetic acid in water was added to each well and vigorously agitated for 30 s. The plate was then read on a plate reader at 590 nm.

Tetracycline and cumate induction

Dual-inducible 293 T cells that were successfully transduced with all three vectors were plated on either 6-well or 12-well plates and allowed to adhere for 16 h overnight. Anhydrotetracycline (C4291, ApexBio Technology) was used as an effector for the Tet-On system and binds the rtTA protein at a much higher affinity than

◀**Fig. 2.** HES3 and PAX3::FOXO1 induction are both reversible. 293Tii cells were plated on 6-well plates at a density of 250,000 cells per well. After overnight adherence, cells were treated with either 50 ng/ml anhydrotetracycline (HES3 induction) or 50 µg/ml cumate (PAX3::FOXO1 induction). Shown are representative images of uninduced cells (A), anhydrotetracycline-induced cells at 24 h post-induction (hpi) and 120hpi (B), and cumate-induced cells at 24hpi and 192hpi (C). Cells were imaged on a Leica DMI microscope with a 10× objective. Brightfield images were exposed for 5 ms. GFP and mCherry images were exposed for 2 s. Scale bar is 500 µm. Cells were then harvested for western blotting. Cells were lysed, and 20 µg of protein was loaded into each well of a 4–15% gradient gel. After transferring to a PVDF membrane, the membrane pieces were blotted with either a HES3 primary antibody (D), FOXO1 primary antibody that recognizes the PAX3::FOXO1 fusion and endogenous FOXO1 (E), or TUBULIN primary antibody (D,E). Relative expression of either HES3 (D) or PAX3::FOXO1 (E) was then quantified using ImageJ (relative to TUBULIN, and presented as the ratio compared to uninduced cells). Each point represents a biological replicate (n = 3 for each condition). The error bars represent the mean ± standard deviation. The p values were calculated using a one-way ANOVA followed by Tukey's multiple comparisons post hoc test. This was repeated three times. HES3 reversibility p-values: uninduced vs 24hpi, p = 0.00006; 24hpi vs 120hpi, p = 0.00006; uninduced vs 120hpi, p = 0.99. PAX3::FOXO1 reversibility p-values: uninduced vs 24hpi, p = 0.00001; uninduced vs 120hpi, p = 0.0003; uninduced vs 192hpi, p = 0.11; 24hpi vs 120hpi, p = 0.019; 24hpi vs 192hpi, p = 0.00009; 120hpi vs 192hpi, p = 0.005. Blots have been cropped from original (D,E). HES3 and associated TUBULIN blot were cut from the same membrane prior to primary antibody hybridization. PAX3::FOXO1 and associated TUBULIN blot were cut from the same membrane prior to primary antibody hybridization. Western blots have been cropped from original and the uncropped blots are presented in Supplemental Fig. 8.

tetracycline⁹. Anhydrotetracycline was dissolved in dimethyl sulfoxide (DMSO, D2650, Sigma-Aldrich) and added in concentrations ranging from 1 ng/mL to 50 ng/mL. The resulting DMSO concentrations were kept to a maximum of 0.1% total volume. A water-soluble cumate solution (QM150A-1, System Biosciences) was used to induce PAX3::FOXO1-T2A-mCherry, and was added in concentrations ranging from 1 µg/mL to 50 µg/mL.

Western blotting

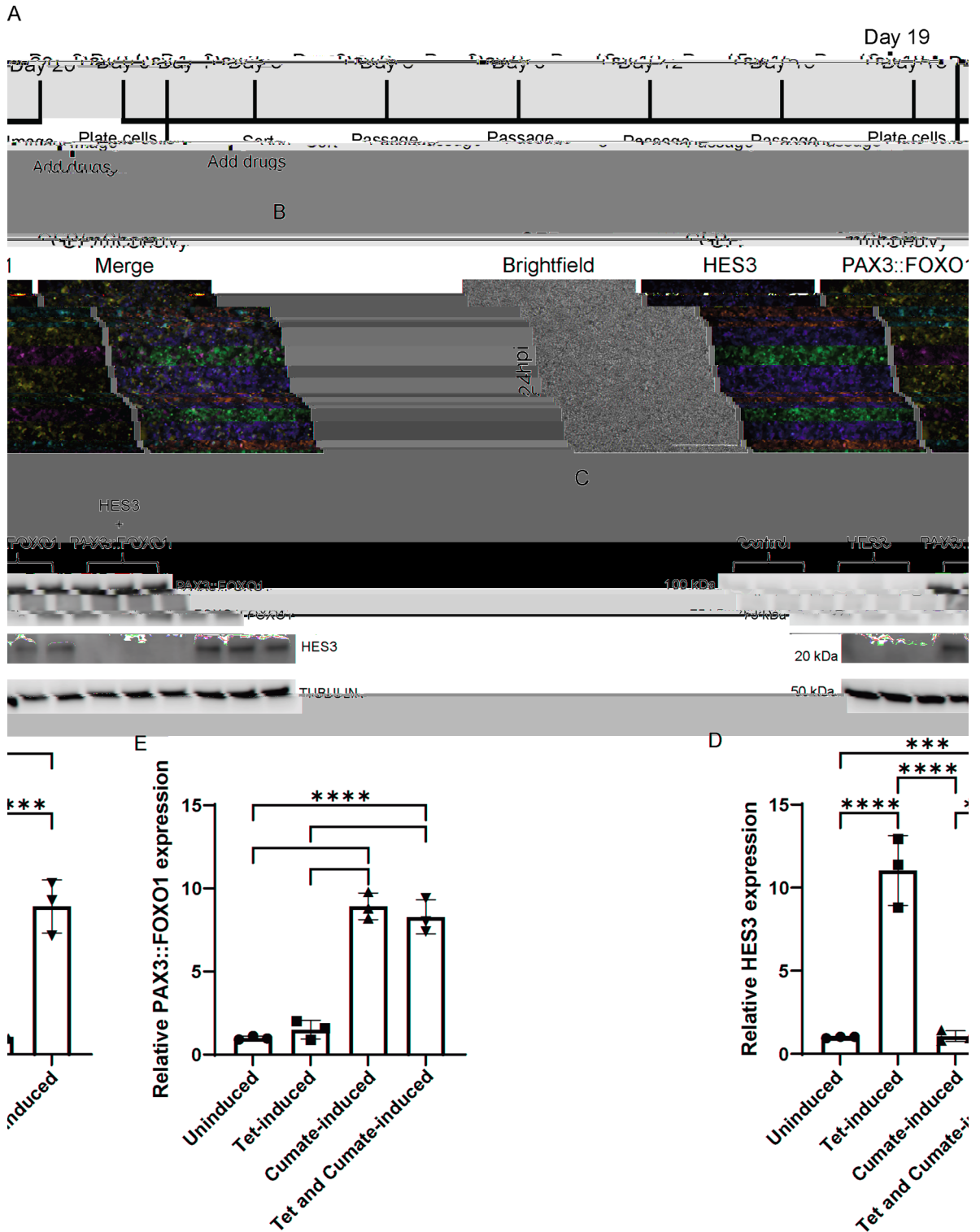
Cells used for western blotting were collected with TrypLE, spun down at 8000xg for 5 min, aspirated of supernatant media, and snap frozen to be stored at - 80 °C. Cells were then lysed with RIPA buffer and 1× protease inhibitor (PI78442, Fisher Scientific) for 2 h on ice. Protein concentration was determined by BCA assay (PI23227, Fisher Scientific). For each sample, 20 µg of protein was loaded into a 4–15% gradient mini-PROTEAN TGX precast protein gel (4561086, Bio-Rad). Gels were run at 150 V in 1× Tris/Glycine/SDS buffer (1610772, Bio-Rad) until the dye front has just run off the gel, approximately 45 min. The samples were then transferred to a PVDF membrane at 400 mA for 2 h at 4 °C in 1× Tris/Glycine buffer (1610771, Bio-Rad). Membranes were then cut at approximately 70 kDa and 37 kDa markers prior to antibody hybridization to prevent potential cross-reaction between HES3, TUBULIN, and FOXO1 antibodies. Membranes were then blocked in casein blocking buffer (PI37528, Fisher Scientific) with 0.05% Tween-20 for 1 h at room temperature. Membranes were then incubated overnight at 4 °C with primary antibodies in fresh casein blocking buffer with 0.05% Tween-20. Primary antibodies used were mouse anti-alpha Tubulin (3873S, Cell Signaling Technologies, RRID: AB_1904178) at 1:1000, mouse anti-HES3 (PCRP-HES3-1A10, Developmental Studies Hybridoma Bank, RRID: AB_2618684) at 0.5 µg/mL, and rabbit anti-FOXO1 (2880S, Cell Signaling Technologies, RRID: AB_2106495) at 1:1000. Then membranes were washed three times for 10 min each in 1× phosphate buffered saline (PBS) with 0.05% Tween-20. Membranes were then incubated at room temperature for 2 h with secondary antibodies in fresh casein blocking buffer with 0.05% Tween-20. Secondary antibodies used were goat anti-mouse horse radish peroxidase (HRP)-conjugated (1706516, Bio-Rad, RRID: AB_11125547) at 1:10,000 and goat anti-rabbit HRP-conjugated (1721019, Bio-Rad, RRID: AB_11125143) at 1:10,000. Membranes were then washed three more times for 10 min each in 1× PBS with 0.05% Tween-20. Membranes were then imaged on a C-DiGit Chemiluminescent Western Blot Scanner (103375-240, VWR) using SuperSignal West Pico PLUS Chemiluminescent Substrate (PI34577, Fisher Scientific) to image TUBULIN and PAX3::FOXO1/FOXO1, and SuperSignal West Atto Ultimate Sensitivity Substrate (38554, Fisher Scientific) to image HES3. While Pico PLUS Chemiluminescent Substrate is not sensitive enough to show membrane edges on a C-DiGit Chemiluminescent Western Blot Scanner, Atto Ultimate Sensitivity Substrate is sensitive enough to show membrane edges on this imager.

Sphere formation

Sphere formation assay was adapted from a previous study¹⁰. Double inducible cells were seeded in 6-well ultralow attachment plates (07-200-601, Fisher Scientific) at 10,000 cells per well in serum free DMEM with GlutaMAX (10569044, Gibco) supplemented with 20 ng/ml bFGF (3718-FB-100, R&D Systems), 20 ng/ml EGF (236-EG-200, R&D Systems), and 1X B27 (17-504-044, Fisher Scientific). Cells were continuously induced with either diluent control, anhydrotetracycline, cumate, or both at time of seeding and for every 4 days for 12 days total. Spheres were imaged and counted manually using a Leica DMIL LED inverted microscope at 12 days after seeding.

Imaging

Images were taken with a Leica DMIL LED microscope with a 10× objective for 2D adherent growth or a 5× objective for 3D sphere growth. Brightfield images had a 5 ms exposure time, GFP a 2 s exposure time, and RFP/mCherry a 2 s exposure time. For Fig. 1, the displayed pixel value range is 300–5000 for GFP and 200–5000



for mCherry. For Fig. 2, the displayed pixel value range is 300–20,000 for GFP and mCherry. For Fig. 3, the displayed pixel value range is 2000–16,000 for GFP and 2000–7000 for mCherry. For Fig. 4, the displayed pixel value range is 1300–65,000 for GFP and 3500–10,000 for mCherry.

Fluorescent-activated cell sorting

Live cell sorting was done using the BD Influx Cell Sorter (BD Biosciences) by BD FACS Software version 1.2.0.142. Cells were sorted into DMEM GlutaMAX growth media supplemented with 10% FBS, 1 × Penicillin/Streptomycin, and 10 mM glutamine. A combination of uninduced transduced cells, tetracycline-induced cells, and cumate-induced cells were separately used to set fluorescence gates. Dual-induced cells were then sorted for both GFP and mCherry fluorescence. The sorted cells were plated on a T-175 flask in additional growth media

◀**Fig. 3.** HES3 and PAX3::FOXO1 can be independently or simultaneously induced in post-sort 293Tii cells. Timeline of experiments for FAC-sorting and post-sort induction (A). Post-sort 293Tii cells were plated on 12-well plates at a density of 250,000 cells per well. After overnight adherence, cells were treated with either 50 ng/ml anhydrotetracycline, 50 µg/ml cumate, or both 50 ng/ml anhydrotetracycline and 50 µg/ml cumate. Cells were imaged at 24 h post-induction (hpi) (B). Cells were imaged on a Leica DMI microscope with a 10× objective. Brightfield images were exposed for 5 ms. GFP and mCherry images were exposed for 2 s. Scale bar is 500 µm. Treated cells were harvested for a western blot and were lysed, and then 20 µg of protein was loaded into each well of a 4–15% gradient gel. After transferring to a PVDF membrane, the membranes were cut and hybridized with either a HES3 primary antibody, FOXO1 primary antibody, or TUBULIN primary antibody (C). Relative expression of HES3 (D) and PAX3::FOXO1 (E) was then quantified. Shown is the ratio of HES3 or PAX3::FOXO1 protein expression normalized to TUBULIN, and presented as the fold-change to no drug treatment (far left on both graphs). Each point represents a biological replicate (n = 3 for each condition). The error bars represent the mean ± standard deviation. The p values were calculated using a one-way ANOVA followed by Tukey's multiple comparisons post hoc test. This was repeated three times. HES3 expression p-values: uninduced vs tet-induced, p = 0.00007; uninduced vs cumate-induced, p = 0.9999; uninduced vs tet- and cumate-induced, p = 0.0004; tet-induced vs cumate-induced, p = 0.00007; tet-induced vs tet- and cumate-induced, p = 0.28; cumate-induced vs tet- and cumate-induced, p = 0.0004. PAX3::FOXO1 expression p-values: uninduced vs cumate-induced, p = 0.000004; uninduced vs tet- and cumate-induced, p = 0.000007; tet-induced vs cumate-induced, p = 0.000006; tet-induced vs tet- and cumate-induced, p = 0.00001. All three blots were cut from the same membrane prior to primary antibody hybridization. Western blots have been cropped from original and the uncropped blots are presented in Supplemental Fig. 9.

with 3 µg/mL blasticidin, 1 µg/mL puromycin, and 300 µg/mL hygromycin and expanded for two weeks without induction prior to any additional experiments. Cells that were transduced and unsorted were used in Figs. 1 and 2, and cells that were sorted were used in Figs. 3 and 4. Both populations were able to generate reproducible induction of HES3 and PAX3::FOXO1.

Image quantification and statistics

Western blots were quantified using ImageJ version 1.53 h (RRID: SCR_003070). Each experiment was repeated 3 times independently, and the number of samples are noted in each figure legend. Statistics were performed using GraphPad Prism 9 (RRID: SCR_002798). p-values for western blot quantifications were calculated using a one-way ANOVA followed by Tukey's multiple comparisons post hoc test.

Results

To generate a dual-inducible cell line, we utilized lentiviruses to transduce HEK293T cells with a series of three different constructs with the Tet-On and Cumate-On systems that each contained a different antibiotic selection marker. These were sequentially introduced in the following order. The first construct contained both the reverse tet transactivator and CymR separated by a T2A sequence (Supplemental Fig S1). This was transduced and cells selected for two weeks with blasticidin. The second construct contained our first Gene of Interest (GOI) cDNA, HES3, separated from an EGFP reporter by a viral T2A sequence and under control of the tet response element (Supplemental Fig S3). This was transduced and cells selected for two weeks with puromycin. The third construct contained our second GOI, PAX3::FOXO1, separated from an mCherry reporter by a T2A sequence and under control of the cumate response element (Supplemental Fig S5). This was transduced and cells selected for two weeks with hygromycin.

After sequentially transducing all three constructs, we tested that expression of HES3 and PAX3::FOXO1 could be induced by anhydrotetracycline or cumate, respectively (Fig. 1A). For HES3 induction, we titrated anhydrotetracycline, an analog of tetracycline that binds the reverse tet transactivator, at 0 ng/ml, 1 ng/ml, 5 ng/ml, 10 ng/ml, 25 ng/ml, and 50 ng/ml. For PAX3::FOXO1 induction, we titrated cumate at 0 µg/ml, 1 µg/ml, 5 µg/ml, 10 µg/ml, 25 µg/ml, and 50 µg/ml. At 24 h post induction (hpi), we were able to see induction of EGFP (Fig. 1B) and mCherry (Fig. 1C). Cells were also collected for western blot, to determine HES3 (Fig. 1D) or PAX3::FOXO1 (Fig. 1E) protein levels at 24 h post induction (hpi). We observed that an increase in drug concentration was consistent with an increase in HES3 (Fig. 1F) and PAX3::FOXO1 (Fig. 1G) protein expression, though there appeared to be a slight leakiness of the cumate repressor in the uninduced cells.

We next wanted to ensure that induction of HES3 and PAX3::FOXO1 expression were reversible. To do this, we induced HES3 and PAX3::FOXO1 expression in separate cell populations. At 24hpi, we imaged the cells and harvested a portion to confirm protein induction by western blot (Fig. 2A–C). Then, we replaced the cell growth media with fresh, drug-free media. From here, we imaged the cells at 48hpi, 96hpi, and 120hpi. By 120hpi, there was virtually no EGFP expression visible, and mCherry expression had decreased as well (Fig. 2B–C). At 120hpi, while there was no HES3 protein expression detectable by western blot (Fig. 2D), there was still detectable PAX3::FOXO1 (Fig. 2E). However, by 196hpi, PAX3::FOXO1 expression decreased back to baseline expression levels (Fig. 2E). This suggests either that PAX3::FOXO1 has a relatively longer half-life than HES3 or that cumate repression takes longer to recover than tetracycline repression, but emphasizes that both systems are reversibly controllable.

While we have confirmed induction of HES3 and PAX3::FOXO1 by fluorescent imaging and protein expression, we also observed a mosaic induction with anhydrotetracycline and cumate (Fig. 1B–C, Fig. 2B–C). We wanted to ensure that our cell population was enriched for inducible cells. To enrich our cell population for those that will successfully induce expression of both HES3 and PAX3::FOXO1, we used fluorescence-activated cell sorting (FAC sorting) to live-sort only cells that are highly fluorescent for both EGFP and mCherry after

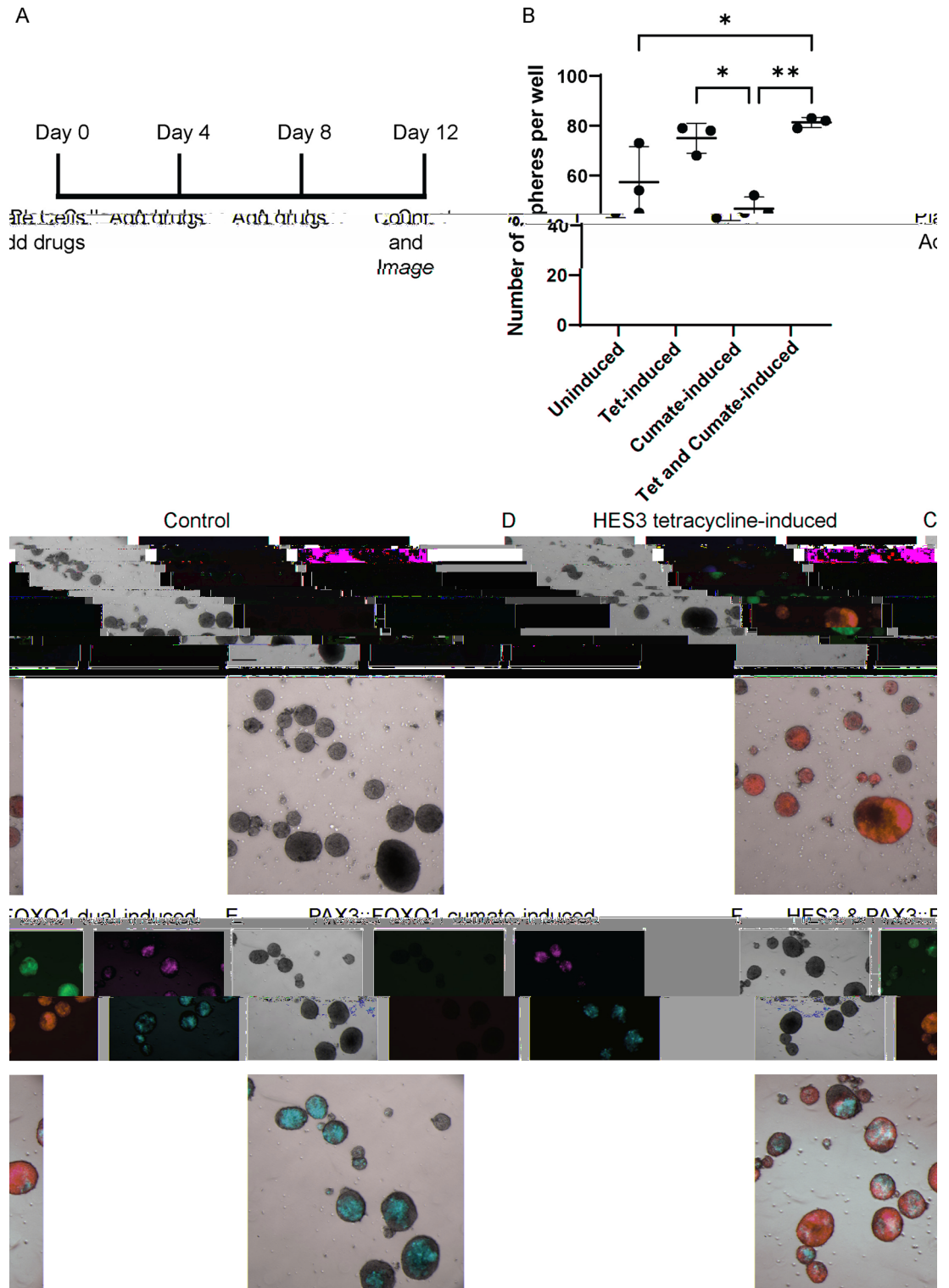


Fig. 4. PAX3::FOXO1-induced cells produce fewer spheres than cells with PAX3::FOXO1 and HES3 dual induction. Sphere formation and non-adherent growth in HEK293T cells is a proxy for oncogenic capacity¹⁰. (A) Timeline of drug addition, counting, and imaging spheres. 10,000 post-sort 293Tii cells were plated on ultralow-attachment 6-well plates, treated with either 0.1% DMSO and 0.1% PBS, 0.1% PBS and 50 ng/ml anhydrotetracycline, 0.1% DMSO and 50 µg/ml cumate, or 50 ng/ml anhydrotetracycline and 50 µg/ml cumate. Every four days after plating, cells were given additional drug at the same concentrations until day 12 (drugs provided on day 0, day 4, and day 8). Spheres were imaged on day 12 on a Leica DMI microscope with a 5× objective. (B) Plotted is the number of spheres per well on day 12. Each point is a technical replicate, the bar represents the mean, and the error bar is the standard deviation. This was repeated an additional two times with similar results. (C–F) Representative images were taken of each condition. Brightfield images were exposed for 5 ms. GFP and mCherry images were exposed for 2 s. Scale bars are 500 µm. Representative images include (C) control-induced cells, (D) HES3 tetracycline-induced cells, (E) PAX3::FOXO1 cumate-induced cells, and (F) HES3/PAX3::FOXO1 dual-induced cells. The p values in B were calculated using a one-way ANOVA followed by Tukey’s multiple comparisons post hoc test. Control vs dual-induced, p = 0.029; tetracycline-induced vs cumate-induced, p = 0.012; cumate-induced vs dual-induced, p = 0.0037.

induction. In this strategy, we induced cells with anhydrotetracycline and cumate on the same cell population for 48 h, along with individually induced cell populations and uninduced transduced cells. We then harvested these cell populations and performed live FAC sorting, with 29.81% of singlets being both EGFP- and mCherry-positive (Supplemental Fig S6). These EGFP and mCherry dual positive cells were collected and expanded in culture for two weeks (including antibiotic selection of blasticidin, puromycin, and hygromycin) to restore tetracycline and cumate repression (Fig. 3A). Then, the dual induction of HES3 and PAX3::FOXO1 was further validated via fluorescent imaging and western blot using the post-sorted cells. For these experiments, we had four conditions of treated cells: water and DMSO only; anhydrotetracycline and water for HES3 induction; cumate and DMSO for PAX3::FOXO1 induction; and anhydrotetracycline and cumate for dual HES3 and PAX3::FOXO1 induction. At 24hpi, we observed comparable levels of HES3 and PAX3::FOXO1 fluorescence following simultaneous induction (Fig. 3B). This was further confirmed by western blot (Fig. 3C), in which the only samples that displayed strong expression of both HES3 (Fig. 3D) and PAX3::FOXO1 (Fig. 3E) were those that received both anhydrotetracycline and cumate. These findings indicate that anhydrotetracycline and cumate induction do not compete with each other, and highlight the discrete control of expression that is available with this system.

To show a functional consequence of HES3 and PAX3::FOXO1 dual expression, we challenged the cells to form spheres as a proxy for tumorigenic capacity¹⁰. A timeline for the experimental strategy is given in Fig. 4A. Cells were plated on day 0 and supplemented with either anhydrotetracycline, cumate, or both. Drugs were added again on days 4 and 8, and spheres were counted and imaged on day 12 (Fig. 4A). Cells induced with only cumate (PAX3::FOXO1) produced fewer spheres than either anhydrotetracycline induction (HES3) or dual induction (PAX3::FOXO1 + HES3) (Fig. 4B), suggesting that HES3 expression is augmenting the PAX3::FOXO1 sphere phenotype. While uninduced cells also formed spheres, there was little to no GFP or mCherry expression (Fig. 4C). Cells induced with either anhydrotetracycline (Fig. 4D) or cumate (Fig. 4E) showed widespread induction of GFP (Fig. 4D) and mCherry (Fig. 4E). In contrast, cells induced with both anhydrotetracycline and cumate had robust induction of both GFP and mCherry (Fig. 4F). These findings suggest that functionally, expression of HES3 is modifying the sphere-forming capacity of PAX3::FOXO1, potentially consistent with its role in promoting more aggressive disease³.

Discussion

Here, we demonstrated a novel strategy of simultaneously utilizing both the Tet-On system and the cumate repressor system in a cell line transduced with three vector constructs. We confirmed that both the Tet-on and cumate systems result in titratable levels of each gene of interest (Fig. 1), and that the expression of both genes is reversible (Fig. 2). Additionally, the systems are simultaneously inducible allowing for controllable expression of both genes of interest in the same cells (Fig. 3). Finally, we showed functional validation of HES3 and PAX3::FOXO1 cooperation using spheres as a proxy for oncogenic capacity, with PAX3::FOXO1 + HES3 dual-induced cells producing more spheres than PAX3::FOXO1 alone (Fig. 4).

PAX3::FOXO1 is the main driver mutation of fusion-positive rhabdomyosarcoma^{11,12}. We found that HES3 is significantly overexpressed in fusion-positive rhabdomyosarcoma patient tumors, and that her3/HES3 knockout in zebrafish supported cancer-related transcriptional profiles^{3,13}. Our zebrafish model has shown PAX3::FOXO1 to be extremely toxic to cells, while HES3 overexpression appears to provide a protective effect against this toxicity³. However, in our inducible 293 T cells, PAX3::FOXO1 does not appear to induce cell death in 2D growth (Fig. 2). It is possible that this is due to the high neural crest and neural signature of HEK293T cells rather than the skeletal muscle lineage¹⁴. Additionally, lack of endogenous HES3 expression or the PAX3::FOXO1 mutation in HEK293T cells made this cell line a strategic choice for a proof-of-concept overexpression model (Supplemental Fig S10). Utilizing this system in human myoblast cells and comparing to our work here in HEK293T cells could provide further information in shared and divergent features of PAX3::FOXO1 and HES3 cooperation depending on the cellular context.

Previous efforts to generate dual-inducible cell lines were typically done via transient transfection of plasmid DNA, allowing for only short-term study^{15,16}. The system described here, similar to the PiggyBac system recently published¹⁷, integrates the lentiviral vectors into the cell genome to generate a stable cell line rather than a transient one. This allows for more long-term and complex studies investigating potential cooperation between the two genes of interest. However, the PiggyBac system utilizes transfection to incorporate plasmids into the genome, which is inherently challenging to integrate into non-dividing and primary cells. Lentivirus-based systems do not share these limitations¹⁸. Therefore, our developed strategy could be more universally applicable to cells that are traditionally challenging to transfect.

Our three-vector strategy to study cooperating genes has a variety of potential applications. Unlike standard overexpression or knockdown studies, this system can be used to investigate timing-dependent relationships between two genes. Additionally, it can be used to look at dose-dependent relationships between cooperating genes in tumorigenesis, a mechanism that has been identified as critical for the function of fusion-oncogenes^{19–21}. This system is flexible and could also be used to incorporate shRNAs, allowing for temporally controlled gene knockdown. With such an approach, the applications could also include a self-contained knockdown/rescue system by using an shRNA against an endogenous gene, and rescuing with that gene or gene variant in the second expression construct. We foresee this new cell model and vector system being used to study a multitude of potential cooperating oncogenic gene pairs, which could provide mechanistic insights and identify novel therapeutic targets for cancer and beyond.

Data availability

Plasmid constructs are in the process of being deposited to Addgene. The data generated in this article are available from the corresponding author by request.

Received: 23 February 2024; Accepted: 26 August 2024

Published online: 05 September 2024

References

- Fang, C., Jiang, B., Shi, X. & Fan, C. Hes3 enhances the malignant phenotype of lung cancer through upregulating cyclin D1, cyclin D3 and MMP7 expression. *Int. J. Med. Sci.* **16**, 470–476. <https://doi.org/10.7150/ijms.28139> (2019).
- Yu, W. *et al.* PD-L1 promotes tumor growth and progression by activating WIP and beta-catenin signaling pathways and predicts poor prognosis in lung cancer. *Cell Death Dis.* **11**, 506. <https://doi.org/10.1038/s41419-020-2701-z> (2020).
- Kendall, G. C. *et al.* PAX3-FOXO1 transgenic zebrafish models identify HES3 as a mediator of rhabdomyosarcoma tumorigenesis. *Elife* <https://doi.org/10.7554/eLife.33800> (2018).
- Bose, M. *et al.* Overexpression of MUC1 induces non-canonical TGF-beta signaling in pancreatic ductal adenocarcinoma. *Front. Cell Dev. Biol.* **10**, 821875. <https://doi.org/10.3389/fcell.2022.821875> (2022).
- Watson, S. *et al.* VGLL2-NCOA2 leverages developmental programs for pediatric sarcomagenesis. *Cell Rep.* **42**, 112013. <https://doi.org/10.1016/j.celrep.2023.112013> (2023).
- MacKay, J. L., Sood, A. & Kumar, S. Three-dimensional patterning of multiple cell populations through orthogonal genetic control of cell motility. *Soft Matter* **10**, 2372–2380. <https://doi.org/10.1039/c3sm52265b> (2014).
- Gossen, M. *et al.* Transcriptional activation by tetracyclines in mammalian cells. *Science* **268**, 1766–1769. <https://doi.org/10.1126/science.7792603> (1995).
- Mullick, A. *et al.* The cumate gene-switch: A system for regulated expression in mammalian cells. *BMC Biotechnol.* **6**, 43. <https://doi.org/10.1186/1472-6750-6-43> (2006).
- Gossen, M. & Bujard, H. Anhydrotetracycline, a novel effector for tetracycline controlled gene expression systems in eukaryotic cells. *Nucl. Acids Res.* **21**, 4411–4412. <https://doi.org/10.1093/nar/21.18.4411> (1993).
- Debeb, B. G. *et al.* Characterizing cancer cells with cancer stem cell-like features in 293T human embryonic kidney cells. *Mol. Cancer* **9**, 180. <https://doi.org/10.1186/1476-4598-9-180> (2010).
- Barr, F. G. *et al.* Rearrangement of the PAX3 paired box gene in the paediatric solid tumour alveolar rhabdomyosarcoma. *Nat. Genet.* **3**, 113–117. <https://doi.org/10.1038/ng0293-113> (1993).
- Barr, F. G. Soft tissue tumors: Alveolar rhabdomyosarcoma. *Atlas Genet. Cytogenet. Oncol. Haematol.* <https://doi.org/10.4267/2042/44650> (2011).
- Kent, M. R. *et al.* Zebrafish her3 knockout impacts developmental and cancer-related gene signatures. *Dev. Biol.* **496**, 1–14. <https://doi.org/10.1016/j.ydbio.2023.01.003> (2023).
- Lin, Y. C. *et al.* Genome dynamics of the human embryonic kidney 293 lineage in response to cell biology manipulations. *Nat. Commun.* **5**, 4767. <https://doi.org/10.1038/ncomms5767> (2014).
- Liu, H. S., Lee, C. H., Lee, C. F., Su, I. J. & Chang, T. Y. Lac/Tet dual-inducible system functions in mammalian cell lines. *Biotechniques* <https://doi.org/10.2144/98244st03> (1998).
- Ma, Y. *et al.* A controlled double-duration inducible gene expression system for cartilage tissue engineering. *Sci. Rep.* **6**, 26617. <https://doi.org/10.1038/srep26617> (2016).
- Sun, W. *et al.* The piggyBac-based double-inducible binary vector system: A novel universal platform for studying gene functions and interactions. *Plasmid* **105**, 102420. <https://doi.org/10.1016/j.plasmid.2019.102420> (2019).
- Karda, R. *et al.* Production of lentiviral vectors using novel, enzymatically produced, linear DNA. *Gene Ther.* **26**, 86–92. <https://doi.org/10.1038/s41434-018-0056-1> (2019).
- Franzetti, G. A. *et al.* Cell-to-cell heterogeneity of EWSR1-FLI1 activity determines proliferation/migration choices in Ewing sarcoma cells. *Oncogene* **36**, 3505–3514. <https://doi.org/10.1038/ncr.2016.498> (2017).
- Bailey, K. M. *et al.* EWS-FLI1 low Ewing sarcoma cells demonstrate decreased susceptibility to T-cell-mediated tumor cell apoptosis. *Oncotarget* **10**, 3385–3399. <https://doi.org/10.18632/oncotarget.26939> (2019).
- Regina, C. *et al.* Negative correlation of single-cell PAX3:FOXO1 expression with tumorigenicity in rhabdomyosarcoma. *Life Sci. Alliance* <https://doi.org/10.26508/lsa.202001002> (2021).

Acknowledgements

We thank Dave Dunway and the Nationwide Children’s Hospital Flow Cytometry Core for providing services to support this study.

Author contributions

Conceptualization: M.K., G.K.; Methodology: M.K., G.K.; Validation: M.K., G.K.; Formal analysis: M.K., A.J., G.K.; Investigation: M.K., A.J., G.K.; Resources: G.K.; Data Curation: M.C., G.K.; Writing – original draft: M.K., G.K.; Writing – review and editing: M.K., A.J., G.K.; Visualization: M.K., G.K.; Supervision: G.K.; Project administration: G.K.; Funding acquisition: G.K.

Funding

This work was supported by NIH/NCI R01 CA272872, an Alex’s Lemonade Stand Foundation “A” Award, and Startup Funds from The Abigail Wexner Research Institute at Nationwide Children’s Hospital to G.C.K. M.K. is funded by the T32 Training Program in Basic and Translational Pediatric Oncology Research grant T32 CA269052. The funders had no role in study design, data collection and analysis, decision to publish, or preparation of the manuscript. Further, the content is solely the responsibility of the authors and does not necessarily represent the official views of the National Institutes of Health.

Competing interests

The authors declare no competing interests.

Additional information

Supplementary Information The online version contains supplementary material available at <https://doi.org/10.1038/s41598-024-71227-3>.

Correspondence and requests for materials should be addressed to G.C.K.

Reprints and permissions information is available at www.nature.com/reprints.

Publisher's note Springer Nature remains neutral with regard to jurisdictional claims in published maps and institutional affiliations.

Open Access This article is licensed under a Creative Commons Attribution-NonCommercial-NoDerivatives 4.0 International License, which permits any non-commercial use, sharing, distribution and reproduction in any medium or format, as long as you give appropriate credit to the original author(s) and the source, provide a link to the Creative Commons licence, and indicate if you modified the licensed material. You do not have permission under this licence to share adapted material derived from this article or parts of it. The images or other third party material in this article are included in the article's Creative Commons licence, unless indicated otherwise in a credit line to the material. If material is not included in the article's Creative Commons licence and your intended use is not permitted by statutory regulation or exceeds the permitted use, you will need to obtain permission directly from the copyright holder. To view a copy of this licence, visit <http://creativecommons.org/licenses/by-nc-nd/4.0/>.

© The Author(s) 2024